

Evolution and origin of Blue Stragglers in 47 Tucanae

Javiera Parada¹ , Harvey Richer¹, Jeremy Heyl¹, Jason Kalirai²
and Ryan Goldsbury

¹Department of Physics and Astronomy, University of British Columbia,
6224 Agricultural Road, Vancouver, Canada
email: jparada@phas.ubc.ca

²Johns Hopkins University Applied Physics Laboratory, 11100 Johns Hopkins Road,
Laurel, Maryland, USA

Abstract. Using data from the core of 47 Tuc we have identified stars in different evolutionary stages in the colour-magnitude diagram, and used the effects of mass segregation on their radial distribution to study the evolution and origin of blue stragglers (BSS). We separate the BSS into 2 samples by their magnitude and find considerable differences in their distribution. Bright BSS are more centrally concentrated with mass estimates over twice the turn-off mass suggesting an origin involving a triple or multiple star system. The distribution of the faint BSS is close to that of the main-sequence (MS) binaries pointing to these stars as their likely progenitors. Using MESA models, we calculate the expected number of stars in each evolutionary stage and compare it with the observed number of stars. Results indicate that BSS have a post-MS evolution comparable to that of a normal star of the same mass and a MS-BSS lifetime of about 200 – 300 Myr.

Keywords. blue stragglers, globular clusters, 47 Tucanae, colour magnitude diagrams, stellar evolution, kinematics and dynamics.

1. Introduction

Star clusters separate stars by their mass through mass segregation: more massive stars will move towards the center of the cluster while less massive stars tend toward larger radii. This process happens on a relaxation time scale, t_{relax} , and makes the position (distance from the center) of the stars in the cluster an indication of their mass. We use the effects of mass segregation to study the origin and evolution of Blue Straggler (BSS) stars in the core of 47 Tuc (see also [Parada et al. 2016b](#)).

BSS appear as an extension of the main sequence (MS); brighter and bluer than the MS turn-off point ([Sandage 1953](#)). 47 Tucanae (NGC 104, 47 Tuc), the second largest and brightest globular cluster in the sky, hosts one of the largest populations of BSS.

The data for this study come from observations made with the *Hubble Space Telescope* using Wide Field Camera 3 (WFC3) to obtain data in the ultraviolet (UV) (GO-12971, PI: H. Richer) and the Advanced Camera for Surveys (ACS) for the data obtain at visible wavelengths (from the ACS Survey of Galactic Globular Clusters, [Sarajedini et al. 2007](#)). The WFC3 data covers a field of radial extent of 160" while the ACS data goes only out to 105".

2. Origin

In old globular clusters there is no evidence of recent star formation; thus for BSS to look younger than the bulk of the stars in the cluster, a rejuvenating process must

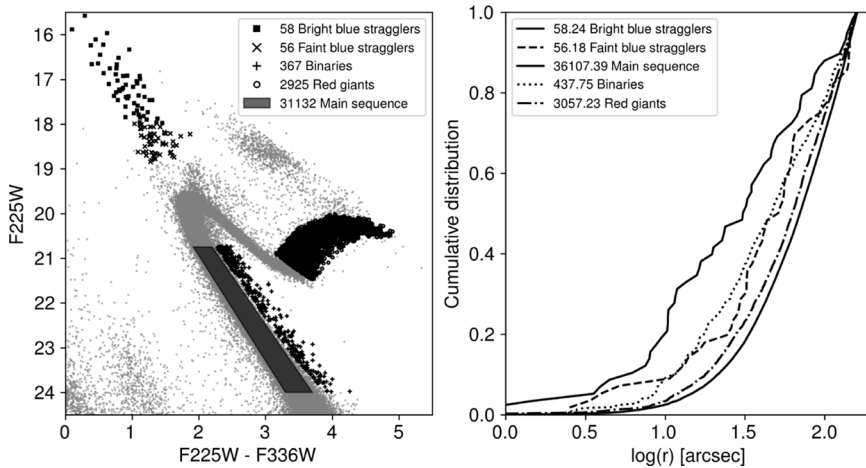


Figure 1. UV colour-magnitude diagram with the selection of stars at different evolutionary stages, the inset shows the number of stars found in each selected region. On the right, the cumulative radial distributions using the number of stars of each type after completeness corrections. There are two solid lines on the plot; the one on the right (least centrally concentrated) represents the MS stars while the other shows the bright BSS.

take place. The BSS formation scenarios are divided in three different categories (Perets 2015): (i) direct collisions of stars (Hills & Day 1976), (ii) stellar evolution of primordial binaries (McCrea 1964), and (iii) dynamical evolution of hierarchical triple systems (Iben & Tutukov 1999). These interactions can result in a single BSS, or a BSS in a system.

To study the possible formation mechanisms responsible for the population of BSS in 47 Tuc, we compare the radial distribution of BSS to the distributions of other groups of stars. We also obtain a dynamical mass estimate which gives an indication of the minimum number of stars involved in the formation process.

We divide the BSS into faint and bright stars. Fig. 1 shows the selected stars for the faint and bright BSS, red giant branch (RGB), MS, and MS binaries. In the right panel of Fig. 1 we draw the cumulative radial distributions for the selected stars.

To obtain an estimate of the dynamical mass, we derived a relation between $\log(M)$ and $\log(R)$ where the cumulative radial distributions reach 20% (R_{20}) and 50% (R_{50}). The equations were obtained through a linear fit using the known masses of three MS regions (the procedure is explained in detail in Parada *et al.* 2016a). This fit is done independently for each field for both R_{20} and for R_{50} , obtaining a total of four equations. Eq. 2.1 shows one example.

$$\log(M_{R_{50}}) = -1.325^{+0.004}_{-0.003} \times \log(R_{50}) + 2.160^{+0.007}_{-0.005} \quad (2.1)$$

2.1. Results and Conclusions

KS-test results indicate no relation between the distributions of the different groups of stars selected, except between the MS binaries and faint BSS with a p-value of 0.76.

Table 1 shows the results of the mass estimates. Difference in mass estimates when using the 105" versus the 160" field is expected for groups of stars that have a wide range of masses. Higher-mass stars migrate toward the center of the cluster; comparing results at R_{20} the 105" field shows higher values because it is closer to the center of the cluster than R_{20} for the 160" field. The same reasoning explains the differences between R_{20} and R_{50} in the same field.

Table 1. Results of the mass estimation (in solar masses) for the groups of stars selected in Figs. 1 and 2 in both the WFC3 complete 160 arcseconds field and the reduced ACS field (105 arcseconds).

	$R \leq 160$		$R \leq 105$	
	M_{R20}	M_{R50}	M_{R20}	M_{R50}
RGB	$0.86^{+0.02}_{-0.02}$	$0.84^{+0.02}_{-0.01}$	$0.88^{+0.03}_{-0.03}$	$0.82^{+0.03}_{-0.04}$
HB	N/A	N/A	$0.88^{+0.07}_{-0.08}$	$0.82^{+0.07}_{-0.12}$
MSBn	$1.15^{+0.04}_{-0.07}$	$1.05^{+0.05}_{-0.10}$	$1.33^{+0.08}_{-0.16}$	$1.35^{+0.13}_{-0.15}$
Bright BSS	$1.64^{+0.06}_{-0.24}$	$1.43^{+0.20}_{-0.56}$	$2.30^{+0.34}_{-0.43}$	$2.27^{+0.83}_{-1.39}$
Faint BSS	$0.93^{+0.09}_{-0.40}$	$0.98^{+0.09}_{-0.25}$	$1.38^{+0.51}_{-0.45}$	$1.26^{+0.26}_{-0.21}$
BSS	$1.47^{+0.20}_{-0.12}$	$1.22^{+0.17}_{-0.15}$	$1.95^{+0.23}_{-0.31}$	$1.44^{+0.15}_{-0.43}$
Evolved BSS	$1.40^{+0.07}_{-0.07}$	$1.38^{+0.07}_{-0.13}$	$1.72^{+0.11}_{-0.14}$	$1.79^{+0.19}_{-0.27}$
Bump	N/A	N/A	$1.52^{+0.28}_{-0.32}$	$2.10^{+1.07}_{-0.67}$
Bright HB	N/A	N/A	$1.45^{+0.27}_{-0.58}$	$1.31^{+0.26}_{-0.51}$

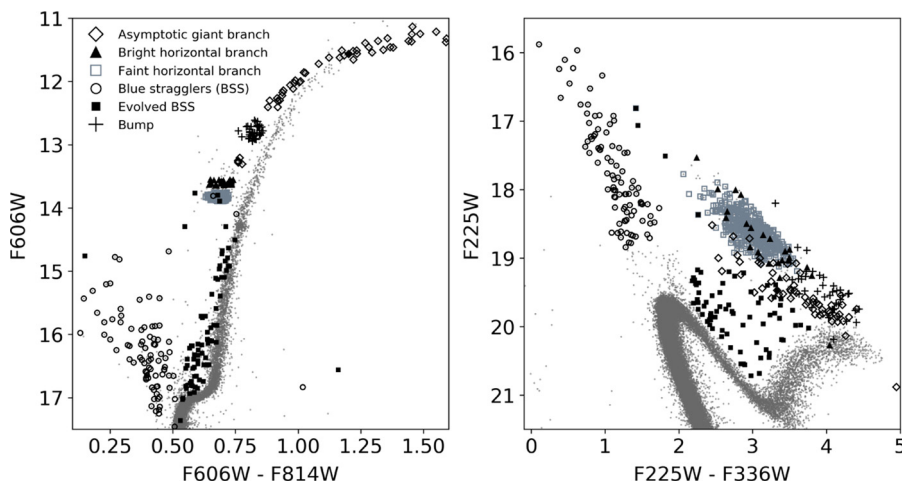


Figure 2. UV (*right*) and visible (*left*) CMD. The stars in the faint and bright HB, AGB, and bump were selected on the visible CMD while the rest are selected in the UV CMD.

Bright blue stragglers are highly concentrated and have higher mass estimates (over twice the turn-off mass), suggesting an origin involving triple or multiple stellar systems. In contrast, faint blue stragglers are less segregated towards the center but still more concentrated than most of the other stars. Their radial distribution and mass estimations are similar to the binaries, pointing to this population as their likely progenitors.

3. Evolution

Post-MS BSS contaminate post main sequence branches with higher mass stars, making the distribution of those stars look more centrally concentrated. [Bailyn \(1994\)](#), [Beccari *et al.* \(2006\)](#) and evolution models ([Parada *et al.* 2016b](#)) link the bright extension of the horizontal branch (HB) and the overabundance of stars in the asymptotic giant branch (AGB) to post-MS BSS. Combining UV and visible data allows us to identify some of the post-MS BSS. These are shown in Fig. 2. We separate the HB into faint and bright

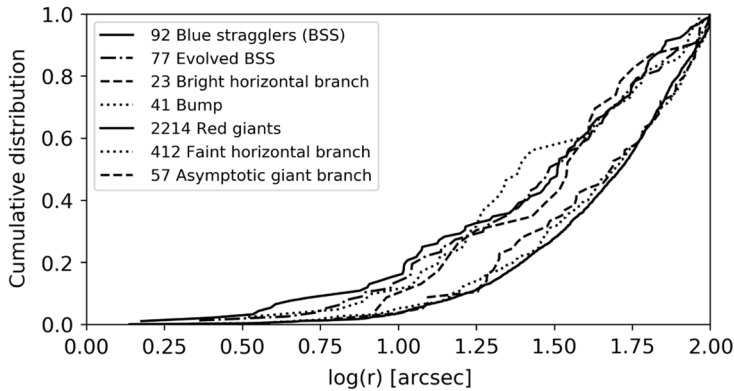


Figure 3. Radial distributions for the stars selected in Fig. 2. The distribution of the RGB stars is included as reference. The RGB, faint HB and AGB stars are represented with line styles already used for other groups of stars but are distinguished as they are well below (less centrally concentrated) the other curves.

objects and the AGB into AGB and bump. The AGB bump is visible only in the visible CMD and stellar evolution models show that the bump is mostly populated by post-MS BSS going up the RGB for the first time. The group of stars referred to as eBSS are BSS that have just left the MS (solid squares in Fig. 2).

3.1. Results and Conclusions

KS-test results for the distributions shown in Fig. 3 and mass estimates (Table 1) point to the BSS, eBSS bright HB and the bump being drawn from the same population with no relation between these and the rest of the groups selected. This result allows us to construct the story of the post-MS evolution of BSS. Following the evolution of normal MS stars we find that the RGB, faint HB and AGB have mass estimates that agree with the turn-off mass ($0.85M_{\odot}$ Ferraro *et al.* 2016). KS-test results cannot reject all these stars being drawn from the same population.

By comparing the observed and expected number of stars in each evolutionary stage, we estimate the BSS main sequence lifetime to be 200-300 Myr. Blue straggler post main sequence evolution is comparable to that of a normal star of the same mass.

References

- Bailyn, C. D. 1994, *AJ*, 107, 1073
 Beccari, G., Ferraro, F. R., Lanzoni, B. & Bellanizi, M. 2006 *ApJL*, 652, L121
 Ferraro, F. R., Lapenna, E., Mucciarelli, A., *et al.* 2016 *ApJ*, 816, 70
 Hills, J. G. & Day, C. A. 1976 *Astrophys. Letters*, 17, 87
 Iben, I., Jr. & Tutukov, A. V. 1999 in *ASP Conf. Ser. 169, 11th European Workshop on White Dwarfs*, ed. S. E. Solheim & E. G. Meistas (San Francisco, CA: ASP), 432
 McCrea, W. H. 1964 *MNRAS*, 128, 147
 Parada, J., Richer, H., Heyl, J., Kalirai, J., Goldsbury, R. 2016b *ApJ*, 830, 139
 Parada, J., Richer, H., Heyl, J., Kalirai, J., Goldsbury, R. 2016a *ApJ*, 826, 88
 Perets, H. B. 2015, in *Ecology of Blue Straggler Stars*, Vol. 413, ed. Boffin, H. M. J., Carraro, G., & Beccari, G., (Berlin: Springer)
 Sandage, A. R. 1953, *AJ*, 58, 61
 Sarajedini, A., Bedin, L. R., Chaboyer, B., *et al.* 2007, *AJ*, 133, 1658